Multi-satellite measurements of large diurnal warming events

Chelle L. Gentemann,[1] Peter J. Minnett,[2] Pierre Le Borgne,[3] and Christopher J. Merchant[4]

Received 18 August 2008; revised 9 October 2008; accepted 13 October 2008; published 20 November 2008.

[1] Diurnal warming events between 5 and 7 K, spatially coherent over large areas (~1000 km), are observed in independent satellite measurements of ocean surface temperature. The majority of the large events occurred in the extra-tropics. Given sufficient heating (from solar radiation), the location and magnitude of these events appears to be primarily determined by large-scale wind patterns. The amplitude of the measured diurnal heating scales inversely with the spatial resolution of the different sensors used in this study. These results indicate that predictions of peak diurnal warming using wind speeds with a 25 km spatial resolution available from satellite sensors and those with 50–100 km resolution from Numerical Weather Prediction models may have underestimated warming. Thus, the use of these winds in modeling diurnal effects will be limited in accuracy by both the temporal and spatial resolution of the wind fields. **Citation:** Gentemann, C. L., P. J. Minnett, P. Le Borgne, and C. J. Merchant (2008), Multi-satellite measurements of large diurnal warming events, *Geophys. Res. Lett.*, *35*, L22602, doi:10.1029/2008GL035730.

1. Introduction

[2] About half of the solar energy reaching the surface of the earth is absorbed by the top 10 m of ocean, often resulting in formation of a diurnal thermocline. The existence of this diurnal warm layer was first described in 1942 [*Sverdrup et al.*, 1942], and has been studied extensively since. Surface temperature deviations greater than 3.0 K, referenced to the foundation temperature (the subsurface temperature below the diurnal thermocline), have been shown [*Gentemann and Minnett*, 2008; *Merchant et al.*, 2008; *Minnett*, 2003; *Yokoyama et al.*, 1995]. These large diurnal events have generally been viewed as isolated occurrences. In this paper, we use independent satellite measurements to verify the existence of large diurnal warming events and examine their spatial and temporal distributions.

[3] A better understanding of diurnal heating of the upper ocean is fundamental to improving the representation of the interactions between ocean and atmosphere in numerical simulations and forecasting of weather and climate. The global sampling offered by satellites provides the best approach to study this component of the earth's climate system, since surface temperature measurements from satellites include the diurnal warming present at the ocean surface, where the interaction with the atmosphere takes place. Failure to account for a diurnal cycle in sea surface temperatures (SSTs) can lead to errors in determining surface fluxes for Numerical Weather Prediction (NWP) and climate models [*Webster et al.*, 1996; *Woods et al.*, 1984].

2. Data

[4] Three independent satellite datasets were used to investigate large diurnal warming events. The AQUA satellite carries both the Advanced Microwave Scanning Radiometer - Earth Observing System (AMSR-E) and the Moderate Resolution Imaging Spectroradiometer (MODIS), providing independent contemporaneous microwave (MW) and infrared (IR) measurements. The AQUA satellite was launched in May 2002 into a polar, sun-synchronous orbit, with a LECT (Local Equator Crossing Time) of 1:30 AM/PM. Over much of the Atlantic Ocean, the geostationary METEOSAT-8 Second Generation (MSG) Spinning Enhanced Visible and Infrared Imager (SEVIRI) provides hourly data. While both MODIS and SEVIRI measure IR radiances, the SEVIRI instrument and viewing geometry is different than MODIS and is therefore independent, as described below.

2.1. AQUA AMSR-E SST

[5] The AMSR-E SST retrieval algorithm [*Wentz and Meissner*, 2000] gives retrievals with a spatial resolution of 25 km and a bias of 0.03 K and standard deviation of 0.42 K when compared to bulk SSTs [*Wentz et al.*, 2003]. A pilot study conducted to determine the accuracy of the AMSR-E SST uncertainties when compared to the skin SST measured by the M-AERI [*Minnett et al.*, 2001] installed on the N/O *L'Atalante* and the NOAA Ship *Ronald H Brown* in the tropical Atlantic Ocean in the summer of 2006 revealed a mean discrepancy of 0.12 K with a standard deviation of 0.39 K (Table 1).

2.2. AQUA MODIS SST

[6] MODIS 11μm SST retrievals are based on the Non-Linear SST algorithm [*Walton et al.*, 1998]. Orbital data are processed into a daily 2.2 km grid covering the SEVIRI region. MODIS SST validation results are given in Table 2. SST retrievals are each assigned a quality flag of 0–4, with 0 being the highest quality. Data must pass 13 different tests to gain a quality flag of 0. If the difference between the retrieved SST and a reference field is >3 K, the quality flag is set to 1. The reference SST test flags undetected clouds as well as diurnal warming events, therefore, for this analysis retrievals with a quality flag of 0 or 1 are used.

2.3. SEVIRI SST

[7] SEVIRI's geostationary orbit provides a unique data set of hourly, 3 km (at nadir) SSTs for the Atlantic region,

[1]Remote Sensing Systems, Santa Rosa, California, USA.
[2]Division of Meteorology and Physical Oceanography, University of Miami, Miami, Florida, USA.
[3]Centre de Météorologie Spatiale, Météo-France, Lannion, France.
[4]School of GeoSciences, University of Edinburgh, Edinburgh, UK.

0094-8276/08/2008GL035730$05.00

from 1 June 2004 onwards. The full resolution SEVIRI SSTs are remapped onto a 0.05° grid using nearest neighbor. The SST retrieval is based on the Non-Linear SST algorithm, using the same coefficients for both day and nighttime data [*Météo-France/CMS*, 2006] and the cloud clearing is based on a multispectral thresholding technique [*Derrien and Le Gléau*, 2005]. In this technique, the temporal variation of measurements is used to identify clouds and could mask areas with rapidly changing diurnal warming. Comparisons to drifting buoys show SEVIRI SSTs to have a negligible bias and standard deviation of 0.5 K [*Le Borgne et al.*, 2006], but errors are correlated in time, such that the random error between consecutive hourly observations is 0.11 K [*Merchant et al.*, 2008]. The local time changes across each hourly SEVIRI image. The Greenwich Mean Time (GMT) referenced measurements were re-mapped to Local Mean Time (LMT) referenced measurements using the longitude and time of each pixel. This process resulted in a new set of hourly maps for the same region, referenced to LMT.

2.4. Calculating the Day-Night SST Difference

[8] The geostationary SEVIRI and polar-orbiting MODIS and AMSR-E have different sampling characteristics. In most regions, the propagation of SST features introduces a relatively small effect and the day-night difference is primarily due to diurnal warming. The location of valid data changes from day to night due to clouds, rain, or location of gaps between successive orbits (swath gaps). To preserve all the daytime measurements, it is important to have a night-time data set with as few missing data as possible. The nighttime SST field for the geostationary sensor, SEVIRI, is an average of all valid data between midnight and 6:00 LMT. For the polar orbiters (MODIS and AMSR-E), nighttime data are the same day descending orbits. Where same-day nighttime data were missing, valid nighttime data from the previous or following day were used.

2.5. Wind speed

[9] Since it has been shown that diurnal variability is sensitive to wind speed variations [*Gentemann and Minnett*, 2008; *Merchant et al.*, 2008] it is important to examine the connection between day-night SST differences and collocated wind speeds. The 6-hourly, 25 km, NASA Cross-Calibrated Multi-Platform (CCMP) winds, a global variational analysis of wind speed [*Atlas et al.*, 1996], are linearly interpolated onto hourly, 2.2 km maps for this study.

3. Frequency and Spatial Variability of Diurnal Warming Events

[10] The Probability Density Functions (PDFs) of SEVIRI ΔT_{dw} at 14:00 LMT for different wind speeds and after averaging to different spatial resolutions are shown in Figure 1. Figure 1a shows that low wind speeds are associated with significant diurnal warming. The distribution peak shifts towards zero and narrows as wind speeds increase. The lowest wind speed class (<1 ms^{-1}) has the highest probability of diurnal events over 1.0 K (60.2%), with the probability of large events decreasing smoothly with increasing wind speed. Although not common, Figure 1 clearly demonstrates that events over 4 K occur. The probability of a diurnal warming event larger than 5 K is 0.5%, 4 K is 3.5%, and 3 K is 14.6% at wind speeds less than 1 ms^{-1}. Variability in diurnal warming is directly related to wind speed, variability in insolation, and variability in wind speed prior to 14:00 LMT SEVIRI measurement. The larger diurnal events likely had low wind speeds for several hours prior to 14:00 LMT, while the smaller diurnal events may have had higher or more variable wind speeds. Figure 1b shows the effect of spatial resolution on the probability of diurnal warming, for wind speeds less than 3 ms^{-1}. As the spatial resolution decreases, the probability of diurnal heating >2 K decreases, while the probability of smaller diurnal events, <2 K, increases. The effect is largest for the lowest spatial resolution. These results clearly demonstrate that spatial resolution will affect measurement of diurnal warming. In the next section several diurnal events are studied using satellite measurements of diurnal warming at different spatial resolutions.

Table 1. Statistics of Comparisons Between AMSR-E SSTs and Coincident M-AERI Skin SSTs in the Tropical Atlantic Ocean

	Mean (K)	STD (K)	N
Ascending (daytime)	0.09	0.45	33
Descending (night)	0.14	0.32	35
Both	0.12	0.39	68

Table 2. Statistics of Comparisons Between the AQUA MODIS SST Retrievals in the Thermal Infrared Atmospheric Transmission Window and Coincident M-AERI Skin SST Measurements

	Mean (K)	STD (K)	N
Ascending (daytime)	0.04	0.59	832
Descending (night)	−0.03	0.53	1261
Both	0.00	0.56	2093

4. Multi-sensor Satellite Retrievals of Diurnal Warming

[11] The SEVIRI day-night differences were examined for spatially coherent large positive differences over 5 K. 595 events were found (Figure 2). Low wind speeds occur more frequently where large diurnal warm events were also found, except in the Tropics where two regions off Africa show frequent low winds, but no large events. Near Angola, cloud cover prevented retrieval of IR SSTs during low wind events. The West African area is known to have aerosol biasing (which cools the IR SSTs) and this may have masked and reduced large warming events. Animations of the daily diurnal events are available in the auxiliary materials.[1] Once these large events were identified in the SEVIRI data, verification using other sensors was completed.

[12] The IR and MW SST retrievals are independent and have different error sources. The primary errors in IR SST retrievals are due to undetected clouds, atmospheric aerosols, and anomalous temperature and water vapor distributions in the atmosphere. The primary errors in MW SSTs are due to calibration errors, high surface wind speeds, near-land side lobe contamination, undetected rain, and satellite

[1] Auxiliary materials are available in the HTML. doi:10.1029/2008GL035730.

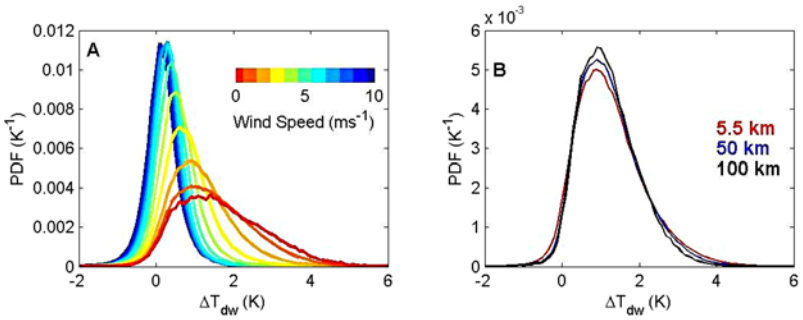

Figure 1. (a) PDF of the SEVIRI day (14:00 LMT) minus night SST difference, ΔT_{dw}, for different wind speeds. (b) PDF of ΔT_{dw} for wind speeds <3 ms^{-1} at different spatial resolutions. As averaging increases, the probability of diurnal events <2 K increases while the probability of larger diurnal events decreases.

attitude errors. Since the sources of errors are independent, coincident observations of similar phenomena lend credibility to the accuracy of the observed behavior. Here MW and IR SSTs are used to examine large diurnal events in the Atlantic Ocean with examples shown in Figures 3 and 4. MODIS and SEVIRI are less complete than AMSR-E due to cloud cover. There are coherent patterns of missing data, most pronounced in the AMSR-E fields, due to gaps between measurements from adjacent orbits. MODIS has a wider swath than AMSR-E and therefore, the gaps between swaths are less apparent in the MODIS SST fields.

[13] Figure 3a shows an area off Southern Africa where low wind speeds have resulted in a large diurnal heating event visible in all the satellite SST difference fields. The warming feature is approximately 1500 km in length and the pattern of warming, which echoes features in the wind speed, is similar in all of the satellite fields. The amplitude of the warming decreases with spatial resolution, from 6.4 K (MODIS), 4.4 K (SEVIRI), to 4.2 K (AMSR-E). The MODIS data have been averaged to a 25 km resolution (denoted M25) and the peak amplitude diurnal heating is 5.1 K. The spatially averaged MODIS peak warming may not equal the AMSR-E peak warming for a number of reasons: the sampling within the MODIS 25 km grid cell may not be spatially complete due to cloud cover or the MODIS grid may not exactly match the AMSR-E footprint (which is elliptical). Figure 3b shows a region off Newfoundland on 1 August 2005. Again, a pattern in low wind speed has resulted in a large diurnal event that is present in all satellite retrievals. The warming extends from 45°N to 50°N and has a maximum of 5.9 K (MODIS), decreasing to 5.2 K (SEVIRI), and further decreasing to 4.1 K (AMSR-E). Figure 3c shows a region off Northwest Africa and Portugal. There are two thin low wind-speed features that result in two long diurnal warming signatures seen in all the satellite retrievals. Figure 3d shows a region off South America, where a low wind speed region has resulted in significant warming. There is a small region separate from the main area of low wind speeds that is also reflected in the diurnal warming pattern seen in MODIS and AMSR-E measurements. That area is masked as cloud in the SEVIRI data. This feature is approximately 1800 km in length and has a diurnal peak of 6.3 K (MODIS). Again the lower resolution sensors measure smaller peak values in warming.

[14] Figures 4a and 4b show 10–11 May 2006, for the same region near the United Kingdom. On 10 May warming was 5.8 K and on 11 May it was 7.1 K, located slightly south of the 10 May peak. While there is some geographical overlap in the warming from one day to the next, the main diurnal warming features are located in different regions, reflecting the change in the patterns of low wind speeds. Warming is 5.6 K and 5.4 K for AMSR-E on the two days. Column C shows a large diurnal feature off the United Kingdom, Spain, and Northern Africa on 4 June 2006. There is also a small diurnal feature in the Mediterranean Sea visible in the MODIS and SEVIRI measurements. It is not in the AMSR-E data as SST retrieval is not possible so close to land. Column D shows another diurnal feature off of Spain on 16 June 2004. The peak warming is 7.0 K (MODIS), 5.4 K (SEVIRI), and 3.9 K (AMSR-E).

[15] The three independent satellite retrievals show remarkable agreement in the location and shape of the diurnal peak, as shown in Figures 3 and 4. Figures 4a and 4d show events with spatial variability that is well tracked by all three sensors. The MODIS diurnal heating fields often show more variability than those of either SEVIRI or AMSR-E, probably due to the high spatial variability in the diurnal warming. Several of the diurnal heating peaks

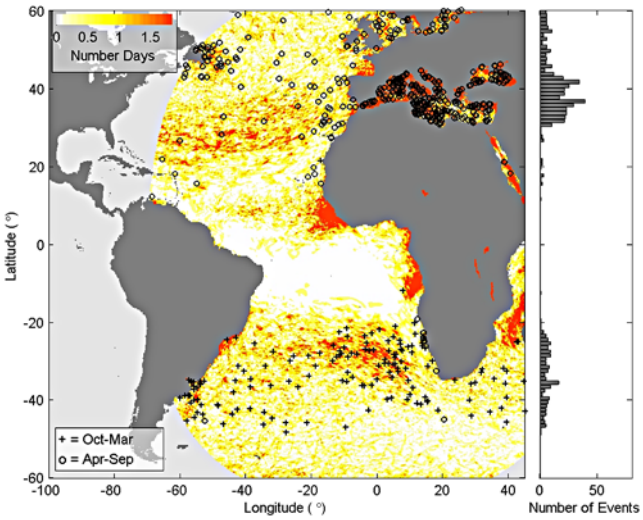

Figure 2. Location of diurnal events over 5 K (black '+' and 'o'). Events generally occur in the boreal (austral) summer. The background color shows the days in a year (on average) that wind speed was <1 ms^{-1} at 14:00 LMT.

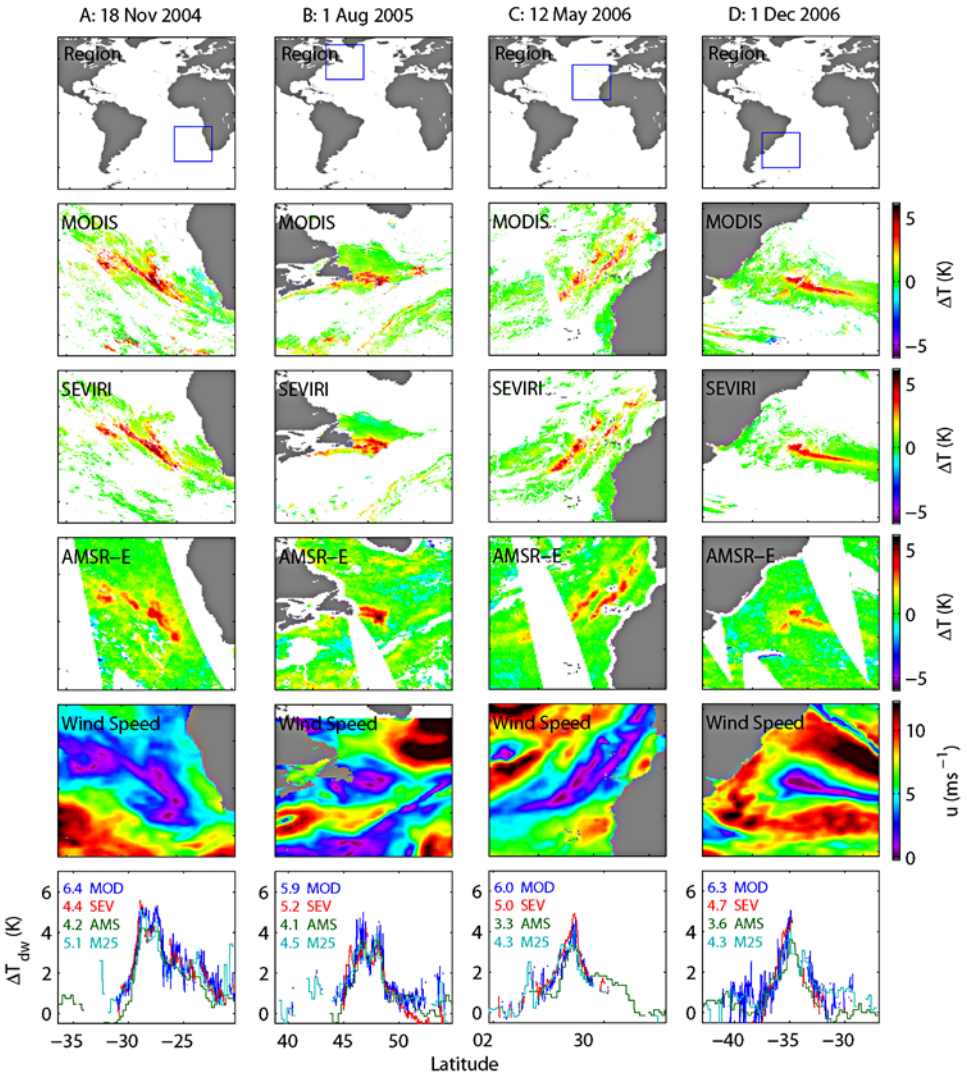

Figure 3. Multiple satellite measurement of diurnal warming events for (a) 18 Nov 2004, (b) 1 Aug 2005, (c) 12 May 2006, and (d) 1 Dec 2006. Location of the areas for which the SSTs are shown, MODIS ΔT_{dw} at 2 km spatial resolution, SEVIRI ΔT_{dw} at 5.5 km, AMSR-E ΔT_{dw} at 25 km, CCMP wind speeds, and the meridional cross-section of SSTs from each sensor through the center of the area, with the numbers giving the peak amplitudes, colored by the data source: MOD is MODIS; SEV is SEVIRI; AMS is AMSR-E, and M25 is MODIS cloud-free data averaged to a 25 km spatial resolution.

show the impact of sensor spatial resolution, with AMSR-E smoothing over the high values. In a few cases, the maximum diurnal heating measured by SEVIRI is larger than for MODIS, or AMSR-E is larger than SEVIRI. This is likely due to sampling as in several cases the diurnal heating peak is masked in SEVIRI data as a result of cloud contamination. Unlike for MODIS, the SEVIRI data do not currently return all measurements whether cloud flagged or not, and it is therefore not possible to relax the quality flag to reveal the diurnal warming.

5. Discussion

[16] These measurements by independent sensors reveal that large diurnal warming events at the ocean surface occur (with peaks >5 K) more frequently then previously thought. The maximum warming measured depended on the spatial resolution of the sensor, but generally the three sensors showed remarkable agreement. Almost all large diurnal events occurred where low wind speeds occur, at latitudes outside 20°S to 20°N. There are several regions where low wind speeds are common in the Tropics, but no large events were found. Tropical SSTs rarely increase above 30°C and there may be a physical mechanism to limit large diurnal events. Studies have explored why Tropical SSTs seldom surpass 30°C (see review by *Webster et al.* [1996]), focusing on nonlinear feedback mechanisms between SST variability and clouds. However, for much of the equatorial Atlantic, Figure 2 indicates that the absence of large diurnal events is because of a lack of very low (<1 ms^{-1}) wind speeds. To ensure that absence of large diurnal events is not due to IR sampling (clouds preventing measurement) or algorithm errors (an underestimation of warming due to high vapor amounts), AMSR-E SSTs were similarly analyzed for large diurnal events (see auxiliary materials). The MW SSTs are able to measure through clouds, are not biased by water

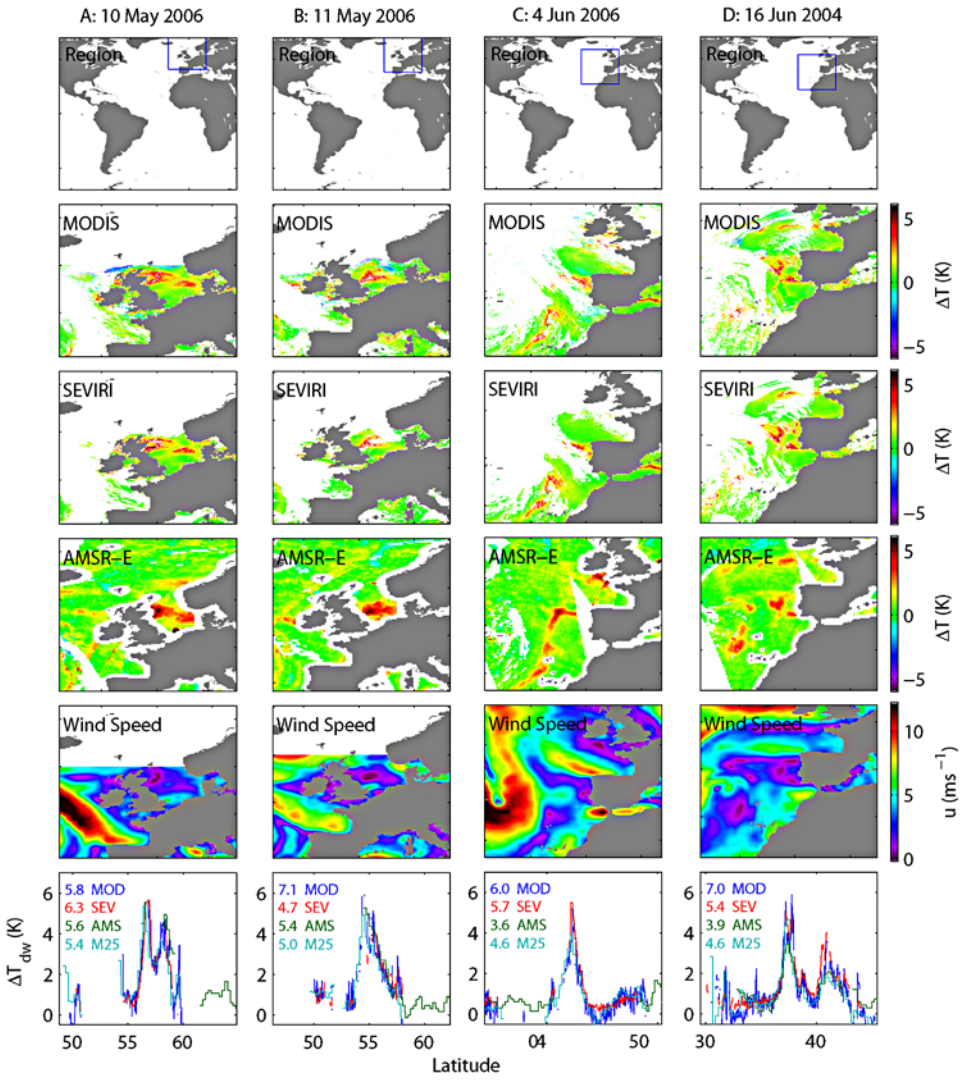

Figure 4. Same as Figure 3 but for (a) 10 May 2006, (b) 11 May 2006, (c) 4 Jun 2006, and (d) 16 Jun 2004.

vapor. They confirm the absence of large diurnal events in the Tropics.

6. Conclusions

[17] Understanding of diurnal warming at the ocean surface is important for improving our estimates of air-sea heat and gas fluxes, optimal assimilation of satellite SST data into analysis systems for weather, ocean state and climate forecasts. Measurements from three satellites show large diurnal heating events extending over large areas. The large diurnal heating signals were found where low winds and high surface insolation occurred in concert. The results presented here indicate a strong dependence of the measured diurnal peak on sensor type, likely due to the sensor's spatial resolution; the probability of measuring diurnal events over 2 K decreases with decreasing spatial resolution. This is the first study to directly compare measurements of diurnal warming events detected using the three main types of spacecraft sensors used to derive SST: infrared and microwave radiometers from polar-orbiters, and an infrared radiometer in geosynchronous orbit. The large diurnal events are independently verified by these different sensors. Although, diurnal warming is frequently present in the Tropics, the observed large diurnal events (greater than 5 K) occurred in extra-tropical regions. These large diurnal events present a new challenge to understanding and modeling air-sea heat and gas fluxes accurately throughout the day.

[18] **Acknowledgments.** This work was supported by NASA contracts NNX08AH99G, NNX07AF83G, NNG04GM56G and NNG04GM57G. Key and Szczodrak, and K. Kilpatrick provided the at-sea M-AERI data used in Tables 1 and 2. The hourly SEVIRI SST data are experimental MF/CMS products from EUMETSAT's OSI-SAF. GHRSST L2P MODIS data were provided by NASA JPL, NASA OBPG, and the University of Miami. GHRSST L2P AMSR-E data were provided by Remote Sensing Systems. Data are available from the GHRSST GDAC (http://ghrsst.jpl.nasa.gov) and the GHRSST LTSRF (http://ghrsst.nodc.noaa.gov). We would like to thank the GHRSST Diurnal Variability Working Group for discussions.

References

Atlas, R. M., R. N. Hoffman, S. C. Bloom, J. C. Jusem, and J. Ardizzone (1996), A multiyear global surface wind velocity dataset using SSM/I wind observations, *Bull. Am. Meteorol. Soc.*, *77*, 869–882.

Derrien, M., and H. Le Gléau (2005), MSG/SEVIRI cloud mask and type from SAFNWC, *Int. J. Remote Sens.*, *26*, 4707–4732.

Gentemann, C. L., and P. J. Minnett (2008), Radiometric measurements of ocean surface thermal variability, *J. Geophys. Res.*, *113*, C08017, doi:10.1029/2007JC004540.

Le Borgne, P., G. Legendre, and A. Marsouin (2006), Operational SST retreival from MSG/SEVIRI data, paper presented at The 2006 EUMETSAT Meteorological Satellite Conference, Eur. Organ. for the Exploit. of Meteorol. Satell., Helsinki.

Merchant, C. J., M. J. Filipiak, P. Le Borgne, H. Roquet, E. Autret, J.-F. Piollé, and S. Lavender (2008), Diurnal warm-layer events in the western Mediterranean and European shelf seas, *Geophys. Res. Lett.*, *35*, L04601, doi:10.1029/2007GL033071.

Météo-France/CMS (2006), *Atlantic Sea Surface Temperature Product Manual Version 1.6*, 49 pp., EUMETSAT Ocean and Sea Ice SAF, Lannion, France.

Minnett, P. J. (2003), Radiometric measurements of the sea-surface skin temperature—The competing roles of the diurnal thermocline and the cool skin, *Int. J. Remote Sens.*, *24*, 5033–5047.

Minnett, P. J., R. O. Knuteson, F. A. Best, B. J. Osborne, J. A. Hanafin, and O. B. Brown (2001), The Marine-Atmospheric Emitted Radiance Interferometer (M-AERI), a high-accuracy, sea-going infrared spectroradiometer, *J. Atmos Oceanic Technol.*, *18*, 994–1013.

Sverdrup, H. U., M. W. Johnson, and R. H. Fleming (1942), *The Oceans: Their Physics, Chemistry, and General Biology*, Prentice-Hall, Englewood Cliffs, N. J.

Walton, C. C., W. G. Pichel, J. F. Sapper, and D. A. May (1998), The development and operational application of nonlinear algorithms for the measurement of sea surface temperatures with the NOAA polar-orbiting environmental satellites, *J. Geophys. Res.*, *103*, 27,999–28,012.

Webster, P. J., C. A. Clayson, and J. A. Curry (1996), Clouds, radiation, and the diurnal cycle of sea surface temperature in the tropical western Pacific, *J. Clim.*, *9*, 1712–1730.

Wentz, F. J., and T. Meissner (2000), *AMSR Ocean Algorithm, Version 2*, 66 pp., Remote Sens. Syst., Santa Rosa, Calif.

Wentz, F. J., C. L. Gentemann, and P. D. Ashcroft (2003), On-orbit calibration of AMSR-E and the retrieval of ocean products, paper presented at the 12th Conference on Satellite Meteorology and Oceanography, Am. Meteorol. Soc., Long Beach, Calif.

Woods, J. D., W. Barkmann, and A. Horch (1984), Solar heating of the oceans-diurnal, seasonal, and meridional variations, *Q.J.R. Meteorol. Soc.*, *110*, 633–686.

Yokoyama, R., S. Tanba, and T. Souma (1995), Sea surface effects on the sea surface temperature estimation by remote sensing, *Int. J. Remote Sens.*, *16*, 227–238.

C. L. Gentemann, Remote Sensing Systems, 438 First Street, Suite 200, Santa Rosa, CA 95401, USA. (gentemann@remss.com)

P. Le Borgne, Centre de Météorologie Spatiale, Météo-France, B.P. 147, F-22302 Lannion CEDEX, France.

C. J. Merchant, School of GeoSciences, University of Edinburgh, The King's Buildings, West Mains Road, Edinburgh EH9 3JZ, UK.

P. J. Minnett, Division of Meteorology and Physical Oceanography, University of Miami, 4600 Rickenbacker Causeway, Miami, FL 33149, USA.